Inorganic Chemistry
Article

Inorg. Chem. **2009,** *48,* 4963–4970 **4963**
DOI:10.1021/ic9002803

Formation and Reactivity of [(tacn)-N-CO-$Re^{III}Br(CO)_2]^+$ in Water: a Theoretical and Experimental Study

Fabio Zobi,*,† Olivier Blacque,† Gideon Steyl,‡ Bernhard Spingler,† and Roger Alberto†

†*Institute of Inorganic Chemistry, University of Zürich, Winterthurerstrasse 190, CH-8057 Zürich, Switzerland and* ‡*Department of Chemistry, University of the Free State, Bloemfontein 9300, South Africa*

Received February 10, 2009

The chemistry of [(tacn)-N-CO-$Re^{III}(CO)_2Br$]X (X = Cl or Br), obtained in good yield from the reaction of *fac*-[(tacn)$Re^{I}(CO)_3$]Br (**1**, tacn = 1,4,7-triazacyclononane) with X_2 in water, is described. The [(tacn)-N-CO-$Re^{III}(CO)_2Br$]X complex (**2** with X = Br^-; **2a** with X = $BrCl_2^-$), which we have previously communicated, is characterized by an unusual three-membered ring acyl amide bond. Complex **2** is stable as a solid but is reactive in aqueous solution. Under basic conditions (1 M NaOH), reductive decarbonylation was observed, and the bis-carbonyl complex [(tacn)$Re^{I}(CO)_2Br$] (**3**) was obtained in quantitative yield. The Br^- ligand in **3** could be replaced by CN^-, giving the neutral complex [(tacn)$Re^{I}(CO)_2(CN)$] (**4**). In acidic media (1 M HBr), complex **2** partially converted to the monocarbonyl μ-oxo bridged dinuclear complex $\{[(tacn)Re^{III}(CO)Br]_2O\}^{2+}$ (**5** as $[PF_6]^-$ salt). Under mild oxidative conditions the trioxo [(tacn)$Re^{VII}O_3$](ReO_4^-) (**6**) was formed almost quantitatively, and small amounts of the uncommon Re^{VI} complex [(tacn)$Re^{VI}O_2Br$](ReO_4^-) (**7**) were identified. Mechanistic investigations at the density functional level of theory (DFT) showed that the elementary steps in the formation of **2** from **1** and **3** from **2** involved reactions of the complexes with hydroxide. The calculated pathway is strongly exothermic (ca. −137 kcal/mol), confirming the energetically and kinetically highly favored formation of **3**. The X-ray structures of **2a** and **3**−**5** are reported and discussed.

Introduction

In the field of metal-based drug discovery and design, Re and Tc play a fundamental role.[1−4] The two isotopes Tc-99m and Re-188 show excellent decay properties for diagnostic (^{99m}Tc, $T_{1/2}$ = 6 h; γ = 140 keV) and therapeutic purposes (^{188}Re, $T_{1/2}$ = 16.9 h; β^- = 2.1 MeV), and both isotopes are readily available from generators. The development of routine procedures for *fac*-$[M(H_2O)_3(CO)_3]^+$ (M = ^{99m}Tc, ^{188}Re)[5] introduced organometallic CO complexes into radiopharmacy. Major research efforts focused on the development of suitable ligand systems for *fac*-$[M(OH_2)_3(CO)_3]^+$ which would allow, via chemical derivatization, to append the radionuclide to a suitable biological vector (e.g., a peptide).

Less attention has been dedicated to the development of other Re and Tc-based cores with only one or two CO ligands. Since cores of the $[M(CO)_{3-x}]^{n+}$ type (M = ^{99m}Tc, ^{188}Re) should have distinctly different electronic properties, new chemical strategies for labeling and targeting via simple substitution reactions or yet unknown chemical derivatization procedures could be enabled. Many compounds with the *cis*-$[Re(CO)_2]^+$ motif are described in the literature, but most of them were prepared from $[ReBr(CO)_5]$ in organic solvents and contained phosphine or Cp ligands.[6−21]

*To whom correspondence should be addressed. E-mail: fzobi@aci.uzh.ch.

(1) Le Bideau, F.; Salmain, M.; Top, S.; Jaouen, G. *Chem.—Eur. J.* **2001**, *7*, 2289–2294.
(2) Jaouen, G.; Top, S.; Vessieres, A.; Alberto, R. *J. Organomet. Chem.* **2000**, *600*, 23–36.
(3) Nguyen, A.; Vessieres, A.; Hillard, E. A.; Top, S.; Pigeon, P.; Jaouen, G. *Chimia* **2007**, *61*, 716–724.
(4) Alberto, R. *Bioorganometallics*; Jaouen, G., ed.; Wiley-VCH: New York, 2005; Chapter 4, pp 97−122.
(5) Alberto, R.; Ortner, K.; Wheatley, N.; Schibli, R.; Schubiger, A. P. *J. Am. Chem. Soc.* **2001**, *123*, 3135–3136.
(6) Casey, C. P.; Sakaba, H.; Hazin, P. N.; Powell, D. R. *J. Am. Chem. Soc.* **1991**, *113*, 8165–8166.
(7) Hubbard, J. L.; Kimball, K. L.; Burns, R. M.; Sum, V. *Inorg. Chem.* **1992**, *31*, 4224–4230.
(8) Hund, H. U.; Ruppli, U.; Berke, H. *Helv. Chim. Acta* **1993**, *76*, 963–75.
(9) Klahn, A. H.; Manzur, C. *J. Coord. Chem.* **1991**, *24*, 101–105.
(10) Aballay, A.; Arancibia, R.; Buono-Core, G. E.; Cautivo, T.; Godoy, F.; Klahn, A. H.; Oelckers, B. *J. Organomet. Chem.* **2006**, *691*, 2563–2566.
(11) Aballay, A.; Godoy, F.; Buono-Core, G. E.; Klahn, A. H.; Oelckers, B.; Garland, M. T.; Munoz, J. C. *J. Organomet. Chem.* **2003**, *688*, 168–173.
(12) Arancibia, R.; Godoy, F.; Garland, M. T.; Ibanez, A.; Baggio, R.; Klahn, A. H. *J. Organomet. Chem.* **2007**, *692*, 963–967.
(13) Carbo, J. J.; Eisenstein, O.; Higgitt, C. L.; Klahn, A. H.; Maseras, F.; Oelckers, B.; Perutz, R. N. *J. Chem. Soc., Dalton Trans.* **2001**, 1452–1461.
(14) Godoy, F.; Klahn, A. H.; Lahoz, F. J.; Balana, A. I.; Oelckers, B.; Oro, L. A. *Organometallics* **2003**, *22*, 4861–4868.
(15) Higgitt, C. L.; Klahn, A. H.; Moore, M. H.; Oelckers, B.; Partridge, M. G.; Perutz, R. N. *J. Chem. Soc., Dalton Trans.* **1997**, 1269–1280.
(16) Klahn, A. H.; Manzur, C.; Toro, A.; Moore, M. *J. Organomet. Chem.* **1996**, *516*, 51–57.
(17) Klahn, A. H.; Oelckers, B.; Godoy, F.; Garland, M. T.; Vega, A.; Perutz, R. N.; Higgitt, C. L. *J. Chem. Soc., Dalton Trans.* **1998**, 3079–3086.
(18) Leiva, C.; Klahn, A. H.; Godoy, F.; Toro, A.; Manriquez, V.; Wittke, O.; Sutton, D. *Organometallics* **1999**, *18*, 339–347.
(19) Leiva, C.; Mossert, K.; Klahn, A. H.; Sutton, D. *J. Organomet. Chem.* **1994**, *469*, 69–77.
(20) Diaz, G.; Klahn, A. H.; Manzur, C. *Polyhedron* **1988**, *7*, 2743–2752.
(21) Klahn, A. H.; Manzur, C. *Polyhedron* **1990**, *9*, 1131–1134.

Published on Web 4/20/2009

Nothing about their behavior in water is known. Furthermore, most of these complexes represent a "dead end" because they are ligand substitution inert, and their poor water solubility limits potential applications.

A few exceptions, however, are known. The $[M(NO)(CO)_2]^{2+}$ core (M = ^{99m}Tc, ^{188}Re) exhibits different properties as compared to the isolobal $[M(CO)_3]^+$ core.[22−27] Owing to the strong π-acceptor capacities of NO^+ together with the additional positive charge, the metal center becomes "harder". In addition, the NO^+ ligand exhibits a stronger trans-effect than CO, eventually allowing a 4-fold substitution with tetradentate ligands. Another example of a water-soluble, air stable, and substitution labile core is *cis*-$[Re(CO)_2(CH_3CN)_2]^+$ as recently described by Kromer et al.[28,29]

As the search for novel, reactive Re- and Tc-based cores for (radio)pharmaceutical applications is a crucial concern in medicinal inorganic chemistry, we have studied the synthesis and reactivity of $[(tacn)\text{-}N\text{-}CO\text{-}Re^{III}(CO)_2Br]^+$ (tacn = 1,4,7-triaza-cyclononane) $\mathbf{2}^+$, obtained in good yield from the oxidative halogenation of *fac*-$[(tacn)Re^{I}(CO)_3]Br$ (**1**). Complex **2**, which we have previously communicated,[30] is characterized by an unusual three-membered ring acyl amide bond and may be considered as a new type of precursor for *cis*-$[Re(CO)_2]^{n+}$ complexes. Herein we describe with a theoretical and experimental approach some basic aspects of the chemistry of **2** in water. Under alkaline conditions, **2** underwent reductive decarbonylation, yielding the stable Re^I complex $[(tacn)Re^{I}(CO)_2Br]$ (**3**) with a *cis*-$[Re(CO)_2]^+$ motif. Theoretical calculations at the density functional level of theory (DFT) for this reaction rationalized the mechanistic pathway. The single Br^- in **3** can be replaced by other ligands. Possible future extension of the chemistry herein described to the corresponding ^{99m}Tc complexes may allow conjugation of the radionuclide to targeting molecules.

Experimental Section

All reagents and solvents were purchased from standard sources and used as received. IR spectra were recorded on a Perkin-Elmer BX II spectrometer in KBr, NMR spectra on a Bruker 500 MHz Avance spectrometer. $[Re^{I}(tacn)(CO)_3]Br$ (**1**) was prepared according to literature.[31] The synthesis of **2** and **3** was previously communicated.[30]

$[(tacn)\text{-}N\text{-}CO\text{-}Re^{III}(CO)_2Br]BrCl_2$ (2a). A 200 mg quantity of **1** (0.42 mmol) was dissolved in 15 mL of water. The solution was placed in an ice bath while stirring, and Cl_2 gas was gently bubbled in for 15 min. Complex **2a** was isolated by filtration as a bright yellow microcrystalline solid, washed with a small amount (ca. 2 mL) of cold water, and dried in vacuum. Yield: 86 mg, 40%. Anal. Calcd for $C_9H_{14}Br_2Cl_2N_3O_3Re_1$ (629.15): C 17.18%, H 2.24%, N 6.68% Found: C 18.02%, H 2.41%, N 7.01%. It was found that the elemental analysis of **2a** corresponds to a mixture of salts of $\mathbf{2a}^+$ with the following ratio: 3 × $\mathbf{2a}^+$ ($BrCl_2^-$) and 1 × $\mathbf{2a}^+$ (Cl^-). For this mixture: Anal. Calcd for $C_{36}H_{59}Br_7Cl_7N_{12}O_{12}Re_4$ (2404.25): C 17.98%, H 2.47%, N 6.99%. ^{1}H NMR, 500 MHz (CD_3CN, δ ppm): 6.51 (s, NH, 2H), 4.02 (m, CH, 2H), 3.63 (m, CH, 2H), 3.41−3.12 (m, CH, 6H), 3.03 (m, CH, 2H). IR (solid state, KBr, cm^{-1}): $\nu_{C\equiv O}$ 2073, 1975; $\nu_{C=O}$ 1765. Crystals suitable for X-ray diffraction were obtained by allowing the filtered solution to stand at 4 °C for 3 h.

$[(tacn)Re^{I}(CO)_2Br]$ (3). The same procedure previously described and starting from **2** can be applied for **2a**.[30] Yield: about 98%. Anal. Calcd for $C_8H_{15}Br_1N_3O_2Re_1$ (451.33): C 21.29%, H 3.35%, N 9.31% Found: C 21.11%, H 3.29%, N 9.22%. ^{1}H NMR, 500 MHz (DMSO, δ ppm): 6.82 (s, NH, 1H), 5.84 (s, NH, 2H), 2.93−2.90 (m, CH, 2H), 2.79−2.75 (m, CH, 5H), 2.65−2.56 (m, CH, 5H). IR (solid state, KBr, cm^{-1}): $\nu_{C\equiv O}$ 1883, 1770. Single crystals suitable for X-ray diffraction were grown at the interphase of a 0.1 M NaOH solution layered on top of a DMSO solution of **2**.

$[(tacn)\ Re^{I}(CO)_2(CN)]$ (4). A 50 mg quantity of **3** (0.11 mmol) was suspended in an aqueous solution of KCN (33 mg, 0.5 mmol in 5 mL of water). The solution was heated to reflux under N_2 for 3 h, allowed to cool and then concentrated to about 1 mL. Complex **4** was then collected by filtration, washed with a small amount of cold water, and dried under vacuum. Yield: 30 mg, 68%. Anal. Calcd for $C_9H_{15}N_4O_2Re_1$ (397.45): C 27.20%, H 3.80%, N 14.10% Found: C 26.89%, H 3.89%, N 13.94%. ^{1}H NMR, 500 MHz (DMSO, δ ppm): 6.79 (s, NH, 1H), 5.81 (s, NH, 2H), 2.93−2.91 (m, CH, 2H), 2.79−2.73 (m, CH, 5H), 2.64−2.56 (m, CH, 5H). IR (solid state, KBr, cm^{-1}): $\nu_{C\equiv O}$ 1880, 1783; $\nu_{C\equiv N}$ 2051. Single crystals suitable for X-ray diffraction were grown by slow diffusion of ether into a methanol solution of the compound.

$\{[(tacn)Re^{III}(CO)Br]_2O\}(PF_6)_2$ (5). A 100 mg quantity of **2** (0.18 mmol) was heated to 40 °C in a 1 M HBr solution (10 mL). The complex slowly dissolved, and the faint yellow solution became green. Heating was continued for 5 h, and then the solution was allowed to cool to r.t. A saturated aqueous solution of NH_4PF_6 was then added (1 mL), and the mixture allowed to evaporate at r.t. for 12 h. Long green needles of **5**, suitable for X-ray diffraction, were then harvested and dried in vacuum. Yield: 12 mg, 11.6%. Anal. Calcd for $C_{14}H_{30}Br_2F_{12}N_6O_3P_2Re_2$ (1152.58): C 14.59%, H 2.62%, N 7.29% Found: C 14.35%, H 2.76%, N 7.18%. IR (solid state, KBr, cm^{-1}): $\nu_{C\equiv O}$ 1900.

$[(tacn)Re^{VII}O_3](ReO_4)$ (6). To 50 mg of **2** (0.09 mmol) in 0.1% trifluoroacetic acid (10 mL) were added 50 μL of a 35% H_2O_2 solution, and the mixture was stirred for 5 h at 25 °C. HPLC-MS analysis of the solution indicated quantitative conversion of **2** to **6**. The colorless solution was allowed to evaporate yielding white crystals of **6** in nearly quantitative yield. Analytical data are in agreement with what previously reported.[31]

Computational Details. Geometry optimizations as well as frequency calculations for all the reactants, products, and transition states were performed at the Density Functional level of theory with the Gaussian03 program package[32] using the hybrid *m*PW1PW91 functional which includes modified Perdew−Wang exchange and Perdew−Wang 91 correlation,[33−36]

(22) Lehaire, M. L.; Grundler, P.; Marti, N.; Merbach, A. E.; Schibli, R. *Chem. Abstr*. **2005**, *230*, U2233–U2233.
(23) Lehaire, M. L.; Grundler, P. V.; Steinhauser, S.; Marti, N.; Helm, L.; Hegetschweiler, K.; Schibli, R.; Merbach, A. E. *Inorg. Chem*. **2006**, *45*, 4199–4204.
(24) Marti, N.; Spingler, B.; Breher, F.; Schibli, R. *Inorg. Chem*. **2005**, *44*, 6082–6091.
(25) Rattat, D.; Schubiger, P. A.; Berke, H. G.; Schmalle, H.; Alberto, R. *Cancer Biother. Radiopharm*. **2001**, *16*, 339–343.
(26) Rattat, D.; Verbruggen, A.; Berke, H.; Alberto, R. *J. Organomet. Chem*. **2004**, *689*, 4833–4836.
(27) Rattat, D.; Verbruggen, A.; Schmalle, H.; Berke, H.; Alberto, R. *Tetrahedron Lett*. **2004**, *45*, 4089–4092.
(28) Kromer, L.; Spingler, B.; Alberto, R. *J. Organomet. Chem*. **2007**, *692*, 1372–1376.
(29) Kromer, L.; Spingler, B.; Alberto, R. *Dalton Trans*. **2008**, 5800–5806.
(30) Zobi, F.; Spingler, B.; Alberto, R. *Dalton Trans*. **2008**, 5287–5289.
(31) Wieghardt, K.; Pomp, C.; Nuber, B.; Weiss, J. *Inorg. Chem*. **1986**, *25*, 1659–1661.
(32) Iyengar, S. S.; Frisch, M. J. *J. Chem. Phys*. **2004**, *121*, 5061–5070.
(33) Adamo, C.; Barone, V. *J. Chem. Phys*. **1998**, *108*, 664–675.
(34) Burke, K.; Perdew, J. P.; Wang, Y. *Electr. Dens. Funct. Theor*. **1998**, 81–111.
(35) Perdew, J. P.; Burke, K.; Wang, Y. *Phys. Rev. B* **1996**, *54*, 16533–16539.
(36) Perdew, J. P.; Burke, K.; Wang, Y. *Phys. Rev. B* **1998**, *57*, 14999–14999.

in conjunction with the Stuttgart/Dresden ECPs (SDD) basis set[37] for the rhenium center and the 6-31 + G(d,p) basis set[38−41] for the remaining atoms. Pure basis functions (5d, 7f) were used in all calculations. Geometries were fully optimized without symmetry restrictions, and the transition state structure was obtained using the QST2 procedure.[42,43] The nature of each optimized stationary point was verified by frequency analyses. For the transition state it was carefully checked that the vibrational mode associated to the imaginary frequency corresponds to the correct movement. In addition, single-point calculations were carried out for all optimized gas-phase geometries using the conductor-like polarizable continuum model (CPCM)[44,45] to compute aqueous solvation free energies. In addition, counterpoise corrections[46,47] were computed to estimate the basis set superposition error for optimized species containing two interacting fragments. Then, the zero-point energies obtained from the gas-phase frequency calculations, the solvent effect corrections, and the basis set superposition errors were included in the given relative energies.

X-ray Crystallography. Suitable crystals were covered with oil (Infineum V8512, formerly known as Paratone N), mounted on top of a glass fiber, and immediately transferred to the diffractometer. Crystallographic data were collected at 183(2) K on an Oxford Diffraction Xcalibur system with a Ruby detector (Mo Kα radiation, λ = 0.7107 Å) using graphite-monochromated radiation. The program suite CrysAlis^{Pro} was used for data collection, semiempirical absorption correction, and data reduction.[48] All structures were solved with direct method using SHELXS-97[49] or SIR-97[50] and were refined by full-matrix least-squares methods on F^2 with SHELXL-97.[49] The structures were checked for higher symmetry with help of the program Platon.[51] CCDC files 719067−719071 contain the supplementary crystallographic data of complexes **2a** and **3**−**5**. These data can be obtained free of charge via www.ccdc.cam.ac.uk/conts/retrieving.html. (They can also be obtained from the CCDC, 12 Union Road, Cambridge CB2 1EZ, U.K. Fax: +44 1223 336033. E-mail: deposit@ccdc.cam.ac.uk.)

Results and Discussion

Synthesis and Structural Analysis. The synthesis and reactions of [(tacn)-N-CO-Re^{III}(CO)$_2$Br]X (**2** with X = Br; **2a** with X = $BrCl_2^-$) are summarized in Scheme 1. Addition of Br_2 (or Cl_2 gas) at r.t. to an aqueous solution of [(tacn)Re^{I}(CO)$_3$]Br (**1**) yielded **2** (or **2a**) within 30 min as an analytically pure, yellow microcrystalline solid in good, isolated yield (≥60% for **2** and about 40% for **2a**).

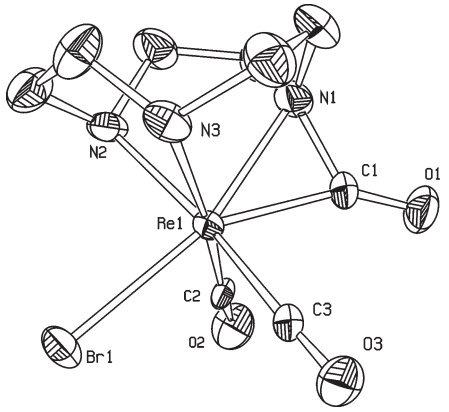

Figure 1. Oak Ridge Thermal Ellipsoid Program (ORTEP) presentation of **2a**$^+$ (50% probability of thermal ellipsoids). The counterion and the hydrogen atoms are omitted for clarity.

Scheme 1. Synthesis and Reactions of Complex **2**[a]

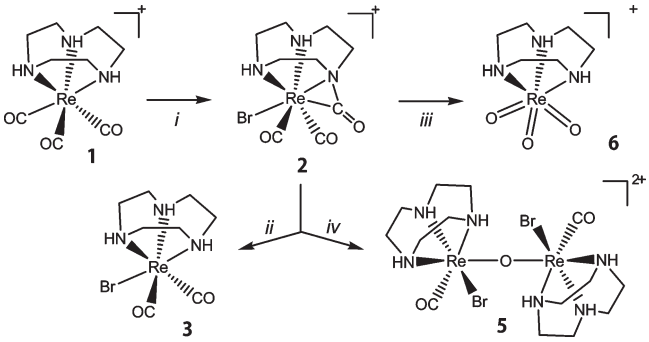

[a] Counter ions are omitted in the scheme. Keys: (*i*) H_2O, 1.5 equiv Br_2, 25 °C, 30 min.; (*ii*) H_2O, 1 M NaOH, 25 °C, 24 h; (*iii*) H_2O, 0.1% trifluoroacetic acid (TFA), H_2O_2, 25 °C 5 h; (*iv*) H_2O, 1 M HBr, 40 °C, 5 h.

Single crystals of **2a** suitable for X-ray diffraction analysis were obtained by allowing the filtrate to stand at 4 °C for another 3 h.

The solid state structure of **2a** is given in Figure 1, and Table 1 lists crystallographic details (bond lengths and angles are given in Supporting Information). Complex **2a** crystallized in the triclinic space group $P\bar{1}$ with two independent molecules per asymmetric unit.

In **2a**, the Re^{III} center is seven coordinate as often observed for d^4 configurations. With the exception of the angles encompassing N1 and C1, all angles around the metal coordination sphere differ slightly from 90°. On average, they are 88.78°(28). Only the N2−N3 bite angle (i.e., the N2−Re−N3 angle, 78.5(4)°) is significantly smaller than average.

Compounds **2** and **2a** behaved in a similar way; thus, unless otherwise noted, the chemistry henceforth described for **2** may be assumed to be the same for **2a**. The oxidative bromination of **1** liberated HBr, and the pH of the aqueous solution dropped to ≈2. If the same reaction was performed in organic solvents, a mixture of products was obtained, indicating that water played a fundamental role in the deprotonation of the tacn ligand and, consequently, in the stabilization of **2**. Compound **2** is stable as a solid, only slightly soluble in water but readily dissolves in organic solvents like methanol, DMSO, or DMF under slow decomposition. ^{1}H NMR, IR spectra, and mass

(37) Andrae, D.; Haussermann, U.; Dolg, M.; Stoll, H.; Preuss, H. *Theor. Chim. Acta* **1990**, *77*, 123–141.
(38) Clark, T.; Chandrasekhar, J.; Spitznagel, G. W.; Schleyer, P. V. *J. Comput. Chem.* **1983**, *4*, 294–301.
(39) Frisch, M. J.; Pople, J. A.; Binkley, J. S. *J. Chem. Phys.* **1984**, *80*, 3265–3269.
(40) Hariharan, P. C.; Pople, J. A. *Chem. Phys. Lett.* **1972**, *16*, 217–219.
(41) Hehre, W. J.; Ditchfield, R.; Pople, J. A. *J. Chem. Phys.* **1972**, *56*, 2257–2261.
(42) Peng, C. Y.; Ayala, P. Y.; Schlegel, H. B.; Frisch, M. J. *J. Comput. Chem.* **1996**, *17*, 49–56.
(43) Peng, C. Y.; Schlegel, H. B. *Isr. J. Chem.* **1993**, *33*, 449–454.
(44) Barone, V.; Cossi, M. *J. Chem. Phys. A* **1998**, *102*, 1995–2001.
(45) Cossi, M.; Rega, N.; Scalmani, G.; Barone, V. *J. Comput. Chem.* **2003**, *24*, 669–681.
(46) Boys, S. F.; Bernardi, F. *Mol. Phys.* **1970**, *19*, 553–566.
(47) Simon, S.; Duran, M.; Dannenberg, J. J. *J. Chem. Phys.* **1996**, *105*, 11024–11031.
(48) *CrysAlisPro Software system*, 171.32; Oxford Diffraction Ltd.: Oxford, U.K., 2007.
(49) Sheldrick, G. M. *Acta Crystallogr.* **2008**, *A64*, 112–122.
(50) Altomare, A.; Burla, M. C.; Camalli, M.; Cascarano, G. L.; Giacovazzo, C.; Guagliardi, A.; Moliterni, A. G. G.; Polidori, G.; Spagna, R. *J. Appl. Crystallogr.* **1999**, *32*, 115–119.
(51) Spek, A. L. *J. Appl. Crystallogr.* **2003**, *36*, 7–13.

Table 1. Crystallographic Data for Compounds **2a** and **3**−**5**

	2a	**3**	**4**	**5**
Formula	$C_9H_{14}Br_2Cl_2N_3O_3Re$	$C_8H_{15}BrN_3O_2Re$	$C_9H_{15}N_4O_2Re$	$C_{14}H_{36}Br_2F_{12}N_6O_6P_2Re_2$
FW	629.15	451.34	397.45	1206.65
T, K	183(2)	183(2)	183(2)	183(2)
space group	$P\bar{1}$	$P2_1/c$	$P2_1$	$P2_1/c$
crystal system	triclinic	monoclinic	monoclinic	monoclinic
Z	4	4	2	4
a, Å	8.0293(2)	10.9948(2)	7.1545(3)	12.7405(2)
b, Å	14.1786(3)	8.3696(2)	11.6007(3)	8.06410(10)
c, Å	14.7420(4)	12.2745(2)	7.3123(2)	29.9394(5)
α, deg	77.459(2)	90	90	90
β, deg	87.532(2)	92.410(2)	108.064(4)	92.4263(14)
γ, deg	89.378(2)	90	90	90
V, Å^3	1636.73(7)	1128.53(4)	576.99(3)	3073.24(8)
d_{calc}, g/cm^3	2.553	2.656	2.288	2.608
R1(wR2)[a]	0.0590 (0.1514)	0.0362 (0.0700)	0.0272 (0.0540)	0.0448 (0.0996)
largest diff. peak/hole (e Å^{-3})	4.869 and −3.025	2.358 and −1.632	1.368 and −0.802	2.449 and −1.992

[a] $[I > 2\sigma(I)]$.

spectrometry indicated the loss of one or more CO ligands from **2**.

If **2** was suspended in a 1 M aqueous NaOH solution, $[(tacn)Re^{I}(CO)_2Br]$ (**3**) was obtained in quantitative yield. Compound **3** is completely stable under aerobic conditions, both as a solid and in solution. To replace Br^- in **3** by an incoming ligand would be an attractive strategy for conjugating **3** to biologically active molecules. Ligand exchange was, however, slow as expected for kinetically stable d^6 complexes. For example, $t_{1/2}$ for $Br^- \rightarrow$ DMSO-d^6 exchange in DMSO-d^6 from **3** to $[(tacn)Re(CO)_2(DMSO\text{-}d^6)]^+$ was about 15 days at r.t. Theoretical calculations indicated the S-binding mode of DMSO to be favored over O-binding by about 5 kcal/mol. If $[(tacn)Re(CO)_2(DMSO\text{-}d^6)]^+$ was left standing for 30 d and then diluted 1:100 in normal non-deuterated DMSO, mass spectrometry did not give any evidence for DMSO exchange after 5 days. Furthermore, the Br^- ligand could neither be replaced by stronger σ-donor ligands such as imidazole or cyanide nor exchanged with soft donors such as thiols if substitution reactions were carried out at r.t. At higher temperatures (≥80 °C, 3 h), however, the bound Br^- could be substituted with CN^- to receive the neutral $[(tacn)Re(CO)_2(CN)]$ complex (**4**) in high yield. Complex **4** was insoluble in water but readily dissolved in organic solvents. The $\nu_{C\equiv O}$ stretching frequencies of **4** (at 1880 and 1783 cm^{-1}) were very similar in energy to those of **3** (see next section) indicating that substitution of Br^- by CN^- did not significantly alter the electronic properties of the metal center.

The solid state structures of **3** and **4** are given in Figure 2. Single crystals of **3** suitable for X-ray diffraction analysis were obtained by layering a 0.1 M NaOH solution on top of a DMSO solution of **2**. Crystals of **4** were obtained from a methanol-diethylether mixture. Complex **3** crystallized in the monoclinic space group $P2_1/c$ with four molecules per unit cell. During the final structure refinement residual electron density was detected between C2−O2 indicating partial disorder between the carbonyl group and the Br^-. This residual electron density was compensated by allowing a 1% occupancy of Br^- at that position. Complex **4** crystallized in the monoclinic space group $P2_1$ with two molecules per unit cell. Bond lengths and angles (Supporting Information) of **4** are similar (within 3σ) to the related $[M(CN)_3(CO)_3]^{2-}$ (M = ^{99}Tc, Re) previously reported.[52]

In comparison to alkaline conditions, the reaction of **2** with acids was different. When **2** was heated in 1 M HBr, the color of the solution turned immediately to green owing to the formation of the monocarbonyl μ-oxo bridged $\{[(tacn)Re^{III}(CO)Br]_2O\}^{2+}$ dimer (**5** as a PF_6^- salt). The complex was isolated as long green needles after the addition of a saturated $[NH_4]PF_6$ solution to the reaction mixture. The solid state structure of **5** is shown in Figure 3. In rhenium chemistry, compound **5** represents one of the very rare examples of a complex showing both a bridging oxo and CO ligands bound to the same metal center. This combination is uncommon since oxo ligands usually prefer high and CO low oxidation states. To our knowledge, no other example was described in literature if cluster compounds with metal−metal bonds are not considered.[53−56]

Complex **5** crystallized in the monoclinic space group $P2_1/c$ with four molecules per unit cell. Metal-oxo bonds (i.e., Re1−O1 and Re2−O1) are essentially identical (within σ) with a length of 1.838(5) Å. If the structure of **5** is compared to all other structures reported in the CCDC and showing a Re−O−Re motif (243 in total, almost all are cluster compounds) the Re−O bond in **5** is significantly shorter than the average (over all structures, 1.933(21) Å). About 70% of the Re−O−Re bond lengths range from 1.883 to 1.980 Å. Deviation on either side of the range are often associated with structures where an oxo of $[O_3Re{-}O]^-$ participates in the oxo bridge (i.e., where the Re-$[O\text{-}ReO_3]^-$ motif is encountered).

Thus, the Re−O−Re bonds in **5** belong to the shortest one known to date. The Re−O−Re bond angle (174.3 (3)°) deviates slightly from linearity and, as a consequence of the bending, the shortest and longest interligand distances are found between Br1 and N5 and C3 and N2,

(52) Kurz, P.; Spingler, B.; Fox, T.; Alberto, R. *Inorg. Chem.* **2004**, *43*, 3789–3791.
(53) Herrmann, W. A.; Serrano, R.; Schafer, A.; Kusthardt, U.; Ziegler, M. L.; Guggolz, E. *J. Organomet. Chem.* **1984**, *272*, 55–71.
(54) Ciani, G.; Sironi, A.; Albano, V. G. *J. Chem. Soc., Dalton Trans.* **1977**, 1667–1670.
(55) Beringhelli, T.; Dalfonso, G.; Freni, M.; Ciani, G.; Moret, M.; Sironi, A. *J. Organomet. Chem.* **1991**, *412*, C4–C6.
(56) Hinrichs, M.; Hofbauer, F. R.; Klufers, P. *Chem.—Eur. J.* **2006**, *12*, 4675–4683.

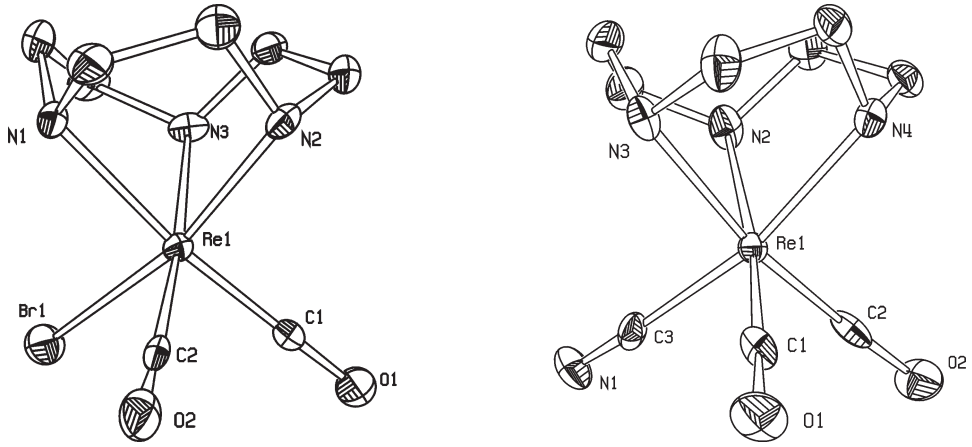

Figure 2. ORTEP presentation of complexes **3** and **4** (50% probability of thermal ellipsoids). The hydrogen atoms are omitted for clarity.

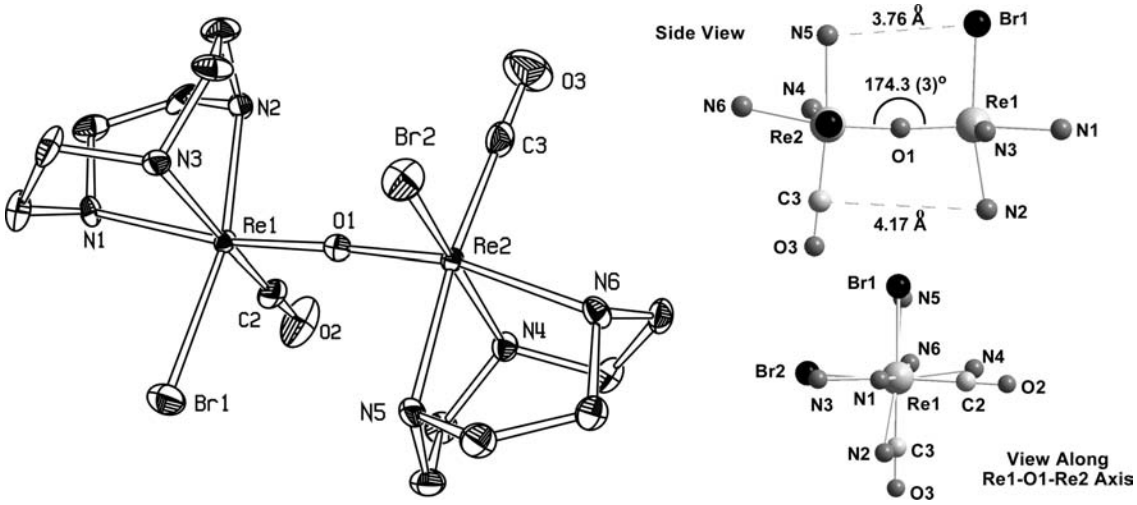

Figure 3. ORTEP presentation of the cation of $\mathbf{5}^{2+}$ (i.e., $\{[(tacn)Re^{III}(CO)Br]_2O\}^{2+}$, 50% probability of thermal ellipsoids). The PF_6^- counterions and the hydrogen atoms are omitted for clarity (left); side view (top) and view along the Re1−O1−Re2 axis for $\mathbf{5}^{2+}$ (bottom, right). Carbon atoms are omitted for clarity.

respectively (see Figure 5, right). The two Re monomers are twisted along the Re−O−Re bond by about 87° with all Re−L bonds (L = atom bound to Re) nearly eclipsing each other (see Figure 5, right). Water molecules connect via an H-bonding network two adjacent cations via N2 and N4.

Complex **5** is stable as a solid, and its IR spectrum showed one single, sharp CO vibration at 1900 cm^{-1} (sharp modes of the counterion are seen at 837 and 558 cm^{-1}). Although being prepared from an aqueous solution, **5** decomposed when redissolved in water. Thorough ^1H NMR analysis of the resulting solution proved difficult because of the presence of multiple set of signals for different complexes containing the tacn ligand. IR spectroscopy and mass spectrometry analysis, however, indicated that conversion of complex **5** consisted in the following: (a) cleavage of the μ-oxo bridge; (b) formation of a monocarbonyl H_2O or $[OH]^-$ complex, and (c) formation of $[(tacn)Re^{VII}O_3]^+$ (**6** as a ReO_4^- salt) in the presence of air and formation of another species with an [Re=O] motif.

When **2** was exposed to air, quantitative conversion to **6** was observed under very mild conditions. One well-defined product as obtained from this reaction was $[(tacn)Re^{VI}O_2Br][ReO4]$ (**7**). Crystals of complex **7** (small red blocks) could be characterized by X-ray structure analysis though the dioxo $[(tacn)Re^{VI}O_2Br]^+$ compound represented only a small fraction of the overall yield. Only a few crystals of **7** could be isolated (yield $<2\%$). We anticipate that **7** might be an intermediate during the oxidative conversion of **2** → **6**. Given the poor quality of the crystals of **7** (final *R* value was 8%) only a model of the molecule, based on structural data, is presented in Figure 4.

Structurally characterized Re^{VI} complexes are very rare and, although no details can be discussed regarding the structure of **7**, we attributed a d^1 configuration to the metal ion based on the following: (a) the Re−O distances which were clearly indicative for terminal oxo rather than hydroxo or water ligands; (b) crystals were grown from strongly acidic conditions (pH ≈ 2), thus, deprotonation of the tacn ligand is unlikely; and (c) crystallographically since it is the anion (ReO_4^-) rather than the cation $[(tacn)Re^{VI}O_2Br]^+$ which was poorly defined in the structure.

Infrared Spectra Analyses. Complexes **1** to **4** showed distinct IR signatures for the ligand CO vibrations (Figure 5). Compound **1** exhibits a sharp symmetric vibration (*sv.*) at 2017 cm^{-1} (A_1) and a broad asymmetric

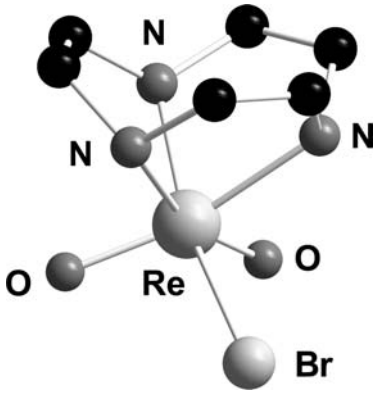

Figure 4. Structure presentation, based on X-ray data, of the cation of [(tacn)$Re^{VI}O_2Br$][ReO4] (**7**).

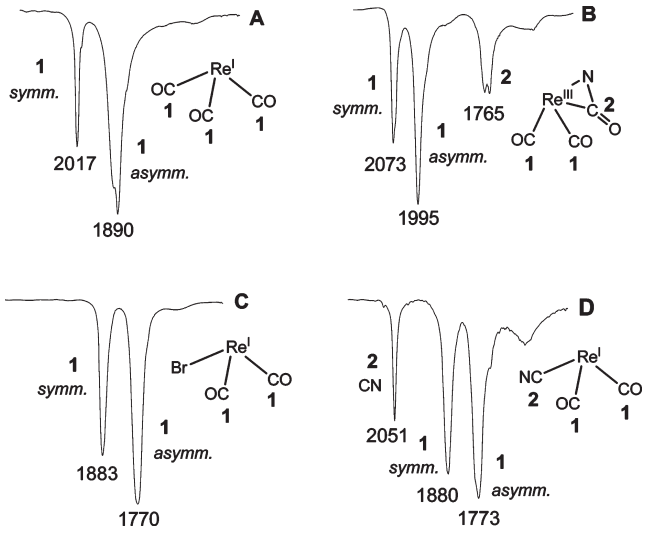

Figure 5. Rhenium-bound CO stretching frequencies in the IR spectra (2200−1500 cm^{-1} region) of complexes **1** (A), **2** (or **2a**, B), **3** (C), and **4** (D). Insets show the Re core in its formal oxidation state. *Symm.* and *asymm.* indicate the symmetric and the asymmetric mode, respectively.

vibration (*asv.*) at 1890 cm^{-1} (E) with a pattern typical for this class of compounds. In **2** (or **2a**), the ν_{CO} bands are blue-shifted by about 60 and 100 cm^{-1} respectively. This hypsochromic shift is consistent with the lower electronic density at the Re^{III} center. The metal displays therefore reduced π-back-donation, and the CO ligands have a more distinct triple-bond character. The opposite is true for **3** and **4** where ν_{CO} bands are both red-shifted by about 130 cm^{-1} as compared to **1** although both, **3** and **4**, are Re^{I}.

The differences in the ν_{CO} stretching frequencies mirror different electronic properties and are rationalized by the presence of 2 COs in **3** (or **4**) vs 3 COs in **1**. The electron density of the metal ion is consequently spread over a lower number of π^* orbitals effectively reducing the C−O bond order in **3** and **4** to a higher degree than in **1**. The increased double-bond character of the CO ligands is then reflected in the bathochromic shift of the ν_{CO} stretching frequencies in the IR spectrum. This analysis finds further support when examining bond distances in the solid state structure of the complexes (see below). The ν_{CO} stretching frequencies of **4** (at 1880 and 1783 cm^{-1}) are very similar in energy to those of **3** indicating that replacing Br^- by CN^- did not significantly alter the electronic properties of the metal.

In the four complexes **1**, **2**, **3**, and **4**, the relative differences of the C≡O bond lengths in the solid state structures correlate well with the relative displacement of the ν_{CO} stretching frequencies in the IR spectra. In this analysis, the average displacements, for both X-ray and IR values, are considered relative to the average values of **1**. For example, the average C≡O bond distance in **1** was calculated as 1.15 Å (see Supporting Information). This value was set as the reference point (i.e., = 0), and the relative average displacement of the same bond in **2**, **3**, and **4** was calculated with respect to the reference point. Thus, on average the C≡O bond distance in **2** is 1.14 Å[30] giving a relative bond displacement of −0.01 Å. Similarly, the average ν_{CO} stretching frequency of **1** (1953.5 cm^{-1}) was set as the 0 reference point in IR analysis.

Figure 6A shows the relative displacement of the Re−C, Re−N, and C≡O bond lengths (Å) of complexes **2**, **3**, and **4** with respect to **1**, and Figure 6B a comparison of the reciprocal relative displacement of the C≡O bond lengths (1/Å) and the relative displacement of the IR C≡O stretching frequencies (for the symmetric, the asymmetric and the average of those, cm^{-1}) of complexes **2**, **3**, and **4** with respect to **1**. It is evident from Figure 6B that the reciprocal relative displacement of the C≡O bond distances followed the same trend of the relative displacement of the IR C≡O stretching frequencies. Although this analysis is straightforward and did not take standard deviations as associated with the X-ray data into consideration, it may provide a basic tool for predicting M−CO bond distances from IR data, and vice versa, within a set of related compounds. Thus, for example, the C≡O bond length of the oxidized form of **3** (i.e., $[Re^{II}Br(tacn)(CO)_2]^+$)[30], which shows the symmetric and the asymmetric CO vibrations at 1999 and 1866 cm^{-1}, respectively, should be in a range between 1.11 and 1.09 Å.

Theoretical Calculations. The synthetic steps outlined in Scheme 1 were generally high yielding but the actual mechanisms for the unexpected conversions **1** → **2** and **2** → **3** were not immediately obvious. To elucidate the mechanism of these reactions, we performed calculations at the density functional level of theory (DFT). The complex $[Re^{III}Br(tacn)(CO)_3]^{2+}$ (**8**) was taken as a starting point for the theoretical calculations. We selected **8** because it is the likely first product of the 2 e^- oxidation of **1** by Br_2 or Cl_2 and therefore an intermediate in the reaction from **1** → **2**. This type of Re^{III} or Tc^{III} cation was, for instance, identified and characterized in oxidative bromination reactions of cyclopentadienyl complexes such as *fac*-$[Re^{I}(C_5(CH_3)_5)(CO)_3]$ and also found in similar reactions of rhenacarboranes species.[57−60] After geometry optimization of complex **8**, its relative energy was set to 0 on the potential energy surface (Figure 7). As the oxidation of **1** by Br_2 was carried out

(57) Blandford, I.; Jeffery, J. C.; Jelliss, P. A.; Stone, F. G. A. *Organometallics* **1998**, *17*, 1402–1411.
(58) Fischer, M. J.; Jelliss, P. A.; Phifer, L. M.; Rath, N. P. *Inorg. Chim. Acta* **2005**, *358*, 1531–1544.
(59) Zobi, F.; Spingler, B.; Alberto, R. *Eur. J. Inorg. Chem.* **2008**, 4205–4214.
(60) Alberto, R.; Schibli, R.; Egli, A.; Abram, U.; Abram, S.; Kaden, T. A.; Schubiger, P. A. *Polyhedron* **1998**, *17*, 1133–1140.

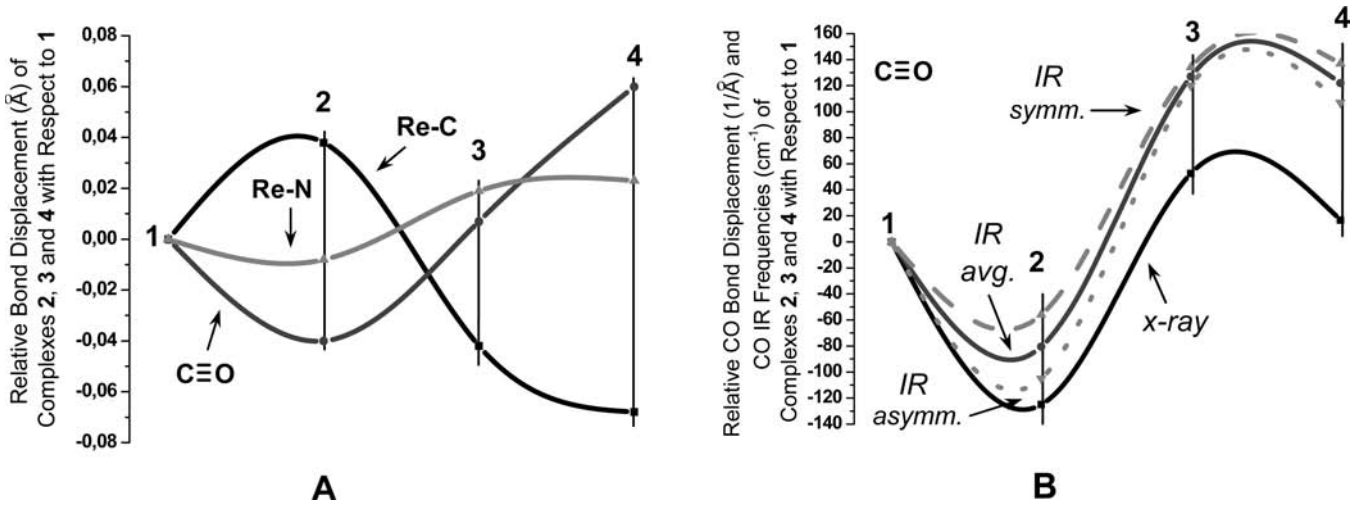

Figure 6. (A) Relative displacement of the Re−C, Re−N, and C≡O bond lengths (Å) of complexes **2**, **3**, and **4** with respect to **1**. (B) Comparison of the reciprocal relative displacement of the C≡O bond lengths (X-ray data, 1/Å) and the relative displacement of the IR C≡O stretching frequencies (IR data, cm^{-1}) of complexes **2**, **3**, and **4** with respect to **1**. Numbers in the graphs correspond to the complexes. The C≡O bond lengths of **2** were taken from reference 30. Only the C1−O1 distance in **3** was considered because of the presence of a disordered Br^- between C2−O2 (see Supporting Information).

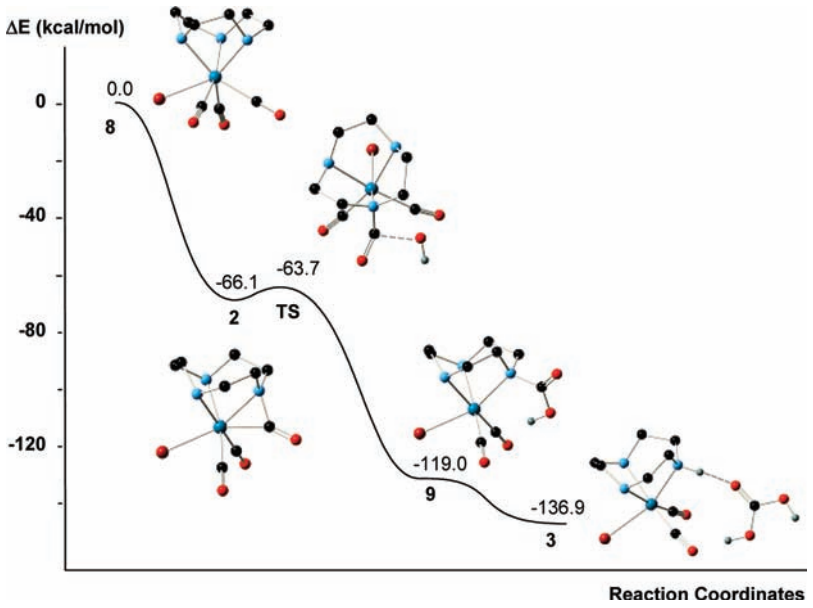

Figure 7. Potential energy surface for the calculated reaction mechanism leading to **3**. Energies are in kcal/mol and relative to the ground-state reactants.

in H_2O, it was reasonable to assume the presence of $[OH]^-$ in solution which served as a base for the deprotonation of N1 (see Figure 1). Indeed, geometry optimization of $\mathbf{8}^{2+}$ in the presence of $[OH]^-$ close to the tacn ligand leads to NH deprotonation. The hydrogen migration from nitrogen to oxygen caused the elimination of a water molecule and a rearrangement leading to the monocationic species $\mathbf{2}^+$, characterized by the formation of one $N-C_{CO}$ bond. The formation of **2** is exothermic by −66.1 kcal/mol as sketched in Figure 7 showing the potential energy trace for the calculated reaction mechanism leading to **3**.

Experimentally, the decarbonylation reaction (i.e., conversion of **2** → **3** in Scheme 1) was performed in an aqueous NaOH solution (pH = 13) in quantitative yield. It is reasonable to assume that the key reaction step involved $[OH]^-$. The geometry optimization of **2** in the presence of $[OH]^-$ in the vicinity of the tacn ligand leads to an attack of $[OH]^-$ to the N-coordinated carbonyl carbon atom of **2**, yielding the neutral carbaminic acid intermediate **9**, formulated as [(tacn)-N-(CO_2H)Re$(CO)_2$Br]. The formation of **9** is once more exothermic by −52.9 kcal/mol relative to **2**. The activation energy corresponding to the transition state **TS2/9** was calculated to be barely 2.4 kcal/mol. Thus, compound **2** could only be isolated since it precipitated rapidly from the reaction solution.

The last step of the decarbonylation was the most difficult one. We have found that decarbonylation of **2** liberates CO_2. This assignment was supported by the observation of a small peak at 8.3 ppm in the ^1H NMR spectrum of the reaction mixture (DMSO-d^6). We assigned this signal to $[H\text{-}CO_3]^-$ resulting from the reaction of CO_2 and H_2O from the solvent. Accordingly, an intramolecular proton migration on **9** as shown in Scheme 2 would be a reasonable transition state

Scheme 2. Two Transition States Considered in the Last Step of the Decarbonylation Reaction (TS9/3)

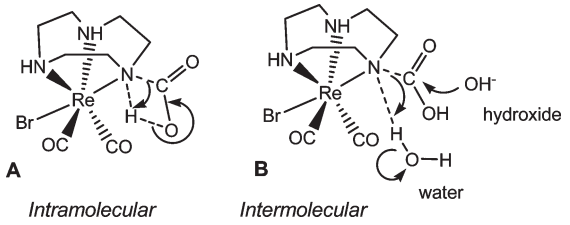

considering the fact that the calculated molecular structure of **9** appeared "prearranged" for this type of mechanism. However, all our attempts to obtain theoretical evidence of the formation of **3** from **9** along this profile failed. Unreasonable structures were obtained which we could not reconcile with the experiments (e.g., hydride migration on Re). Thus, we considered an intermolecular mechanism which turned out to be correct (Scheme 2).

Accordingly, the last step of the decarbonylation required an attack of $[OH]^-$ onto the carboxylate carbon which weakens the N−C bond. Simultaneously, the carbaminic nitrogen abstracts one proton from water. The reaction yields the final product **3** and results in the elimination of hydrogen carbonate. The formation of **3** is thermodynamically favored relative to **9** by −17.9 kcal/mol and confirms that the calculated pathway is highly favored, both energetically and kinetically.

An interesting finding from the theoretical calculations was the reductive decarbonylation from **2** → **3** which proceeds via the neutral carbaminic acid intermediate **9**. Substituting the reactive $[OH]^-$ in the first step with a primary aliphatic amine should yield urea-type derivatives opening new strategies for conjugating these metal complexes to amine groups from biomolecules. To this end, we have attempted such a derivatization with benzylamine in water, methanol, or DMSO but, in all cases, exclusively **3** was obtained. Obviously the primary amine did not attack the N-coordinated carbonyl carbon atom in **2**. We could not detect a urea-type bond being formed during these reactions (by liquid IR). This indicated that the amine acts rather as a base, promoting the formation of $[OH]^-$ entering then the mechanism as described above. The proposed formation of a urea motif, however, should be possible under rigorous anhydrous conditions and is currently pursued in our laboratory.

Conclusions

The [(tacn)-N-CO-$Re^{III}(CO)_2$Br]Br complex **2** is a useful precursor for the synthesis of mono- and bis-carbonyl complexes of Re^I and Re^{III}. Because of its well behaved reactivity, **2** is a convenient starting material for achieving Re^I complexes such as **3**, comprising the *cis*-[$ReBr(CO)_2$] motif in which the Br^- can be substituted for further biologically relevant ligands. Although the exchange kinetics of **3** were slow, higher temperatures promoted the substitution of Br^- in **3** by cyanide, exemplifying a route for site directed functionalization of the basic complex framework. Theoretical calculations assessed a neutral carbaminic acid intermediate in the conversion of **2** → **3**. Initial attempts to tarp this intermediate with a primary amine did not succeed yet; however, more anhydrous conditions should enable urea-type Re^I complexes and, thus, the syntheses of medicinally useful complexes. The isolation of the uncommon dinuclear Re^{III} complex **5** points toward novel reactivity patterns which will be explored in the future.

Acknowledgment. We thank the Swiss National Science Foundation (Ambizione PZ00P2_121989/1) for financial support.

Supporting Information Available: Crystallographic tables for compounds **1**−**5**. This material is available free of charge via the Internet at http://pubs.acs.org.